RAMAN CALIBRATION OF SHOCKED Ca-, Mg- AND Fe-CARBONATES. L. Coloma[1], J. Aramendia[1], I. Población[1], F. Alberquilla[1], G. Arana[1], J. Huidobro[1], K. Castro[1], J. M. Madariaga[1], E. Clavé[2], J. R. Johnson[3], G. López-Reyes[4], J. A. Manrique[4], S. K. Sharma[5], A. Ollila[6], R. C. Wiens[7], S. M. Clegg[6], A. Cousin[8], O. Gasnault[8] and the SuperCam team. [1]University of the Basque Country UPV/EHU, Department of Analytical Chemistry, P.O. Box 644, 48080 Bilbao, Spain (leire.coloma@ehu.eus), [2]DLR - Institute of Optical Sensor Systems, Berlin, Germany, [3] John Hopkins University Applied Physics Laboratory, USA, [4]ERICA, U. Valladolid, Spain, [5]Univ. Hawaii, Honolulu, HI, USA, [6]Los Alamos National Laboratory, Los Alamos, NM 87545, USA, [7]Purdue Univ., West Lafayette, IN, USA, [8]IRAP CNRS, CNES, 31400 Toulouse, France.

Introduction: Carbonates have been detected on Mars by the Perseverance, Spirit and Curiosity rovers [1, 2, 3]. These minerals were also detected in Martian meteorites, for example in the Northwest Africa (NWA) 1950 [4] or in the Allan Hills (ALH) 84001 [5]. Some of the carbonate minerals detected in meteorites are shocked altered phases that are identified easily with Raman spectroscopy and morphology observations [4].

Extreme conditions can alter carbonate minerals and here we explore whether new high-pressure polymorph phases may be formed. In this work, four carbonate minerals are considered: calcite ($CaCO_3$), siderite ($FeCO_3$), magnesite ($MgCO_3$) and dolomite ($CaMg(CO_3)_2$). In Figure 1, the high pressure polymorphs of each carbonate and the pressure at which they are formed are represented. Depending on the carbonate, one to six different phases have been reported.

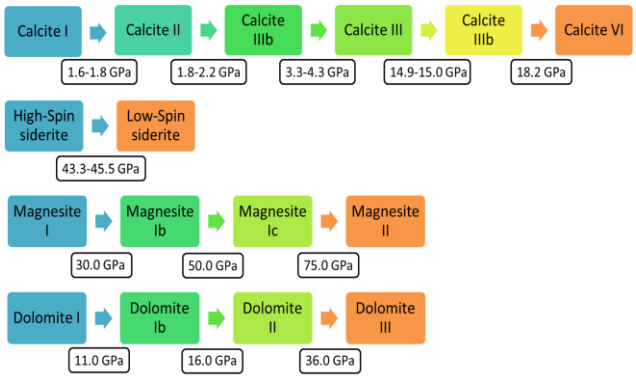

Figure 1. High pressure polymorphs of calcite, siderite, magnesite and dolomite [6-10]

Raman spectra of these four carbonates are well studied at ambient conditions, but the spectra of the high-pressure polymorphs are not known so well. In this work, calibration curves for the different high-pressure phases of calcite, siderite, magnesite and dolomite were made combining literature data and representing the main Raman band position of each carbonate at different pressures.

Methodology: To produce the calibration curves, data from literature were analyzed studying the position of the main Raman band for calcite, siderite, dolomite and magnesite at high pressures. With that dataset, a calibration curve for each type of high pressure polymorph was constructed, in the form:

$$y = k_0 + k_1 . x$$

where y is the Raman wavenumber of the maximum for the most intense vibration carbonate band and x is the pressure in GPa units. For each calibration curve, the residual values on wavenumbers (difference between the observed maximum of the main Raman band of carbonate and the calculated one by the calibration plot) at each pressure were calculated and the Dixon's Q test was used to evaluate the probable presence of outliers on such residuals. When outliers were detected, the observed data were rejected in order to improve the quality of the obtained calibration curves, based on the r^2.

Results and discussion: Figures 2, 3 and 4 summarizes the calibration curves obtained. For calcite, data from calcite I [11, 12], calcite II [13, 14], calcite IIIb [15] and calcite III [12, 15] were available in the literature. Calcite I and II have only one main Raman band whereas in the case of calcite IIIb and calcite III the main Raman band is split in two bands. The Raman band position was found for the two high pressure polymorphs (High-Spin and Low-Spin) of siderite [16, 17, 18]. For magnesite, Raman wavenumbers positions were also found for magnesite I [19, 20, 12], magnesite Ib [19] and magnesite Ic [19]. In contrast, in the case of dolomite, only values for dolomite I were available on theexisting literature [21, 22].

As seen in Figures 2-4, there are differences in the behavior of the calibration curves obtained for each high pressure polymorph as they have different slopes. Depending on the pressures at which carbonate was exposed, a different calibration curve has to be used.

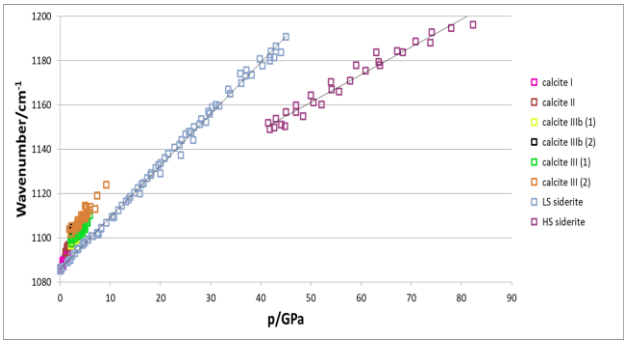

Figure 2. Calibration curves for calcite I, calcite II, calcite IIIb, calcite III, LS siderite and HS siderite.

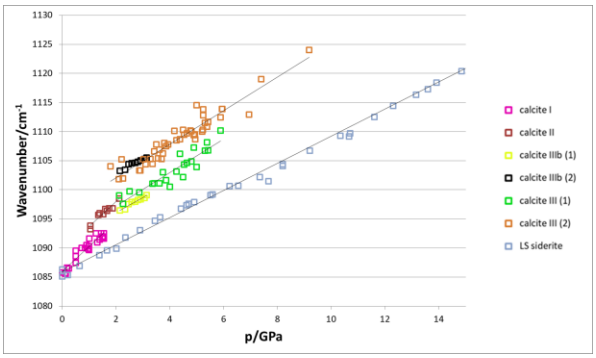

Figure 3. Zoom in the region of 0 to 14 GPa of the previous Figure 2.

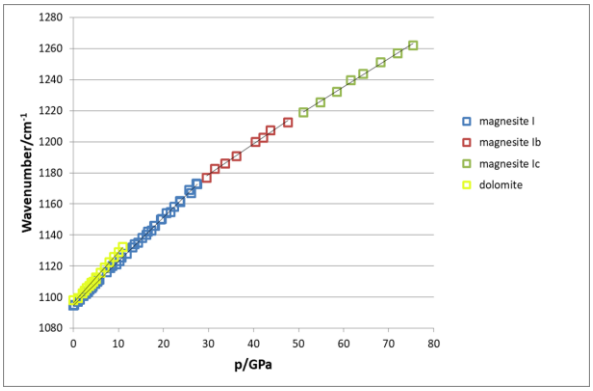

Figure 4. Calibration curves of magnesite I, magnesite Ib, magnesite Ic, and dolomite.

Perseverance will start in few sols (Martian days) the in-situ observations of the Jezero crater rim where the possibility to detect high pressure carbonate rocks is really high. The calibration curves proposed in this work will be tested, together with other SuperCam observations (RMI, LIBS and VISIR) to identify the presence and geochemical characteristics of possible shocked carbonates. Using the elemental values obtained by LIBS on targets that confirmed the presence of carbonate as seen by Raman and VISIR, and taking into account the other minerals detected by the analytical techniques onboard Perseverance, it is possible to identify which metal-carbonate(s) is(are) present calculating the amount of each element according to the stoichiometric modeling [23].

Conclusions: The high-pressure carbonates calibration curves obtained are very important for the near future in the Mars2020 mission, because of the possible identification of shocked carbonates in the Jezero crater rim. For this reason, it is very important to complete the calibration curves for the high-pressure polymorphs for which no literature values were found. For future work, laboratory analyses can provide data to complete these calibrations.

Acknowledgments: This work has been financially supported through the PAMMAT project (Grant No. PID2022-142750OB-I00) and the SIGUE-Mars network (Grant No. RED2022-134726-T) funded by the MCIN/AEI/10.13039/501100011033/FEDER-UE, Spain, as well as the Strategic Project "Study of Alteration Processes in Terrestrial and Planetary Materials" (Grant No. UPV/EHU PES21/88), funded by the UPV/EHU.

References: [1] Morris R. V. et al. (2010) *Science*, *329*, 5990. [2] Scheller E. L. et al. (2022) *LPSC 2022* Abstract 20220003568. [3] Bennett K. A. et al. (2022) *J. Geophys. Res. Planets*, *128*, 1, e2022JE007185. [4] Coloma L. et al. (2022) *J. Raman Spectrosc.*, *53*, 12, 2068-2085. [5] Bridges J. C. et al. (2019) *Volatiles in the Martian Crust*, *5*, 89-118. [6] Pippinger T. et al. (2015) *Phys. Chem. Miner.*, *42*, 29-43. [7] Belkofsi R. et al. (2018) *Modelling Simul. Mater. Sci. Eng.*, *26*, 065004. [8] Efthimiopoulos I. et al. (2017) *Phys. Chem. Miner.*, *44*, 465-476. [9] Zhao C. et al. (2021) *Am. Min.*, *106*, 367-373. [10] Müller J. et al. (2016) *Am. Min.*, *101*, 2638-2644. [11] Yuan X. et al. (2020) *J. Raman Spectrosc.*, *51*, 1248-1259. [12] Farsang S. et al. (2021) *Am. Min.*, *106*, 581-598. [13] Yuan X. et al. (2018) *Mineral. Mag.*, *83*, 2, 191-197. [14] Fong M. Y. and Nicol M. (1971) *J. Chem. Phys.*, *54*, 2, 579-585. [15] Pippinger T. et al. (2015) *Phys. Chem. Minerals*, *42*, 29-43. [16] Liang W. et al. (2018) *Phys. Chem. Minerals*, *45*, 831-842. [17] Zhao C. et al. (2020) *Minerals*, *10*, 1142. [18] Müller J. et al. (2016) *Am. Min.*, *101*, 2638-2644. [19] Zhao C. et al. (2021) *Am. Min,*. *10*6, 367-373. [20] Liang W. et al. (2018) *Phys. Chem. Minerals*, *45*, 423-434. [21] Gillet P. et al. (1993) *Phys. Chem. Minerals*, *20*, 1-18. [22] Efthimiopoulos I. et al. (2017) *Phys. Chem. Minerals*, *44*, 465-476. [23] Madariaga, J.M. et al., *This Conf.*